Author(s): Gendy, Chris; Rautiainen, J. Mikko; Mailman, Aaron; Tuononen, Heikki M.

Title: Low-valent Germanylidene Anions : Efficient Single-site Nucleophiles for Activation of Small Molecules

Year: 2021

Version: Accepted version (Final draft)

Please cite the original version:

Gendy, C., Rautiainen, J. M., Mailman, A., & Tuononen, H. M. (2021). Low-valent Germanylidene Anions : Efficient Single-site Nucleophiles for Activation of Small Molecules. Chemistry : A European Journal, 27(58), 14405-14409. https://doi.org/10.1002/chem.202102804

Chemistry–A European Journal
Communication
doi.org/10.1002/chem.202102804
Chemistry Europe
European Chemical Societies Publishing

Low-Valent Germanylidene Anions: Efficient Single-Site Nucleophiles for Activation of Small Molecules

Chris Gendy,*[a] J. Mikko Rautiainen,[a] Aaron Mailman,[a] and Heikki M. Tuononen*[a]

Abstract: Rare mononuclear and helical chain low-valent germanylidene anions supported by cyclic (alkyl)(amino) carbene and hypermetallyl ligands were synthesised by stepwise reduction from corresponding germylene precursors via stable and isolable germanium radicals. The electronic structures of the anions can be described with ylidene and ylidone resonance forms with the Ge–C π-electrons capable of binding even weak electrophiles. The germanylidene anions reacted with CO_2 to give μ-CO_2-κ*C*:κ*O* complexes, a rare coordination mode for low-valent germanium and inaccessible for the related neutral germylones. These results implicate low-valent germanylidene anions as efficient single-site nucleophiles for activation of small molecules.

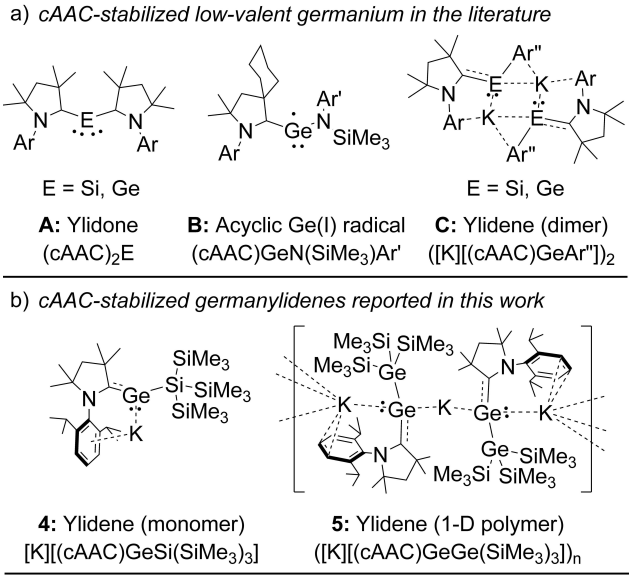

Figure 1. Low-valent germanium species stabilised by cyclic (alkyl)(amino) carbenes (cAACs).

Mononuclear complexes of germanium have garnered attention as congeners of transition metals in bond activation processes. The most intensely studied chemistries in this class involve Ge^{II}-Ge^{IV} reactivity in which germanium functions primarily as a single-site ambiphile via a Lewis acidic p-orbital and an electron pair.[1–11] More recently, ylidones $(cAAC)_2E$ (cAAC = cyclic (alkyl)(amino)carbene; E = Si, Ge) **A** (Figure 1) featuring electron-rich Group 14 elements formally in oxidation state zero have been put to the fore. Akin to transition metals, increased nucleophilicity at the metalloid is critical to effect bond activation. These low-valent species are supported by ancillary ligands combining good σ-donor quality and capacity for accepting back-donation.[12–15] As such, carbenes and carbenoids are commonly employed in designs which range from simple monodentate ligands[16–21] to more exotic chelating[22–28] and pincer-type frameworks.[29–31] Despite the growing collection of ylidones, their chemistry is still in its infancy and dominated by coordination of Lewis acids and oxidative addition reactions with polar substrates.[26,30,32–35] Advancements in this regard include isolated incidents of frustrated Lewis pair reactivity with H_2,[26] activation of CO_2,[36] and metal-ligand cooperation.[31]

Contrasting the number of neutral ylidone compounds, related germanium-centred anions are scarce. This is surprising given the popularity of low-valent anionic aluminium nucleophiles[37–43] and is perhaps associated with the limited profile of anionic ligands in the chemistry of zero-valent germanium. Replacing a neutral cAAC unit in germylone **A** for a charge bearing amido ligand allows the stabilization of radicals **B**.[44] Although electrochemical evidence suggests that anions may be obtained by reduction of **B**,[44] the only known example, **C**, has been independently reported and its reactivity remains unexplored.[45]

Aiming to develop the chemistry of low-valent germanium further, we deployed the electronic stabilization afforded by Me_2-cAAC (1-(2,6-diisopropylphenyl)-3,3,5,5-tetramethylpyrrolidine-2-ylidene, 2,6-diisopropylphenyl = Dipp) in combination with sterically encumbering hypermetallyl ligands E-$(SiMe_3)_3$ (E = Si, Ge) that are not significantly π-withdrawing; cf. the cAAC ligand and aryl group in **A** and **C**, respectively. This led to the synthesis of potassium salts of germanylidene anions $[(Me_2\text{-cAAC})GeE(SiMe_3)_3]^-$ via corresponding germanium-centred radicals. Subsequent computational analyses and reactivity

[a] Dr. C. Gendy, Dr. J. Mikko Rautiainen, Dr. A. Mailman, Prof. Dr. H. M. Tuononen
Department of Chemistry, NanoScience Centre
University of Jyväskylä
P.O. Box. 35, 40014 Jyväskylä (Finland)
E-mail: chris.c.gendy@jyu.fi
heikki.m.tuononen@jyu.fi

Supporting information for this article is available on the WWW under https://doi.org/10.1002/chem.202102804

studies showed the electronic structures of $[(Me_2\text{-cAAC})GeE(SiMe_3)_3]^-$ (E = Si, Ge) to reside between ylidene and ylidone extremes, and the anions are able to function as efficient nucleophiles even with weak electrophiles, such as CO_2.

The reaction of $(Me_2\text{-cAAC})GeCl_2$, **1**,[20] with a half equivalent of $Mg[E(SiMe_3)_3]_2(THF)_2$[46,47] at −78 °C in THF (Scheme 1) yielded hypermetallyl germylene complexes **2a** (E = Si) and **2b** (E = Ge). Complexes **2** can be isolated in good yields by crystallization from hot heptane and stored for several months at −20 °C. NMR spectroscopy showed the expected resonances for **2** with ^{13}C chemical shifts for the carbenic carbon at 248.0 and 249.8 ppm for **2a** and **2b**, respectively. These signals are in-line with that of $(Me_2\text{-cAAC})GeCl_2$ (245.2 ppm),[20] but significantly deshielded compared to related N-heterocyclic carbene (NHC) complexes $(NHC)GeClE(SiMe_3)_3$ (E = Si, 173.1 ppm; E = Ge, 174.0 ppm).[48]

The molecular structures of **2** were confirmed by single crystal X-ray diffraction, revealing pyramidal geometry around germanium (Figures S18 and S19). The measured Ge–C bond lengths (2.015(2) and 2.025(3) Å in **2a** and **2b**, respectively) are slightly shortened as compared to $(NHC)GeClSi(SiMe_3)_3$ (2.093(3) Å),[48] indicating Ge→C back-bonding typical of cAAC-supported complexes that is also evident in their calculated HOMOs (Figure S32). Despite the different atomic properties of germanium and silicon,[49,50] varying the hypermetallyl ligand does not lead to significant structural or spectroscopic changes between **2a** and **2b** (cf. **4** and **5**, see below).

Radical complexes **3** were prepared by reduction of germylenes **2** using an excess of 10 % potassium naphthalenide ($[K][C_{10}H_8]$) at −78 °C (Scheme 1). Recrystallization from pentane at −30 °C afforded analytically pure products. Room temperature EPR spectra of **3** (pentane, Figure S16) show broad singlets with $g \approx 2.0$ and linewidths of approximately 40 G owing to the coupling of the mostly germanium-centred (50 %, Figure S33) unpaired electron to ^{14}N (~3.5 G) and ^{1}H nuclei on the methyl groups of both Me_2-cAAC and $SiMe_3$ (0.1–3.4 G). The redox properties of **3** were characterised by cyclic voltammetry ($[NBu_4][PF_6]$ in THF, Figure S17), with both species showing an electrochemically reversible one-electron reduction attributed to the formation of anions **4** and **5** ($E_{1/2} = -2.02$ V and −2.07 V vs. Fc/Fc^+ for **3a** and **3b**, respectively).

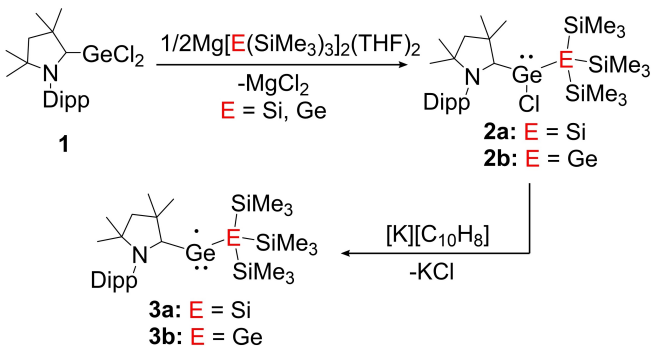

Scheme 1. Synthesis of germylenes **2** and radicals **3** (Dipp = 2,6-*i*$Pr_2C_6H_3$).

Single crystal X-ray diffraction studies of **3** show two-coordinate germanium in a classic bent-geometry (Figures S20 and S21). Buried volume estimates suggest well protected metal coordination pockets, as imposed by Dipp and $SiMe_3$ substituents (V_{bur} = 74.7 and 74.5 % in **3a** and **3b**, respectively).[51–54] Measured Ge–C bond lengths in **3** are comparable to those reported for **B** ((1.993(3) and 1.985(1) Å in **3a** and **3b**, respectively, vs. 1.986(2) Å in **B**)[44] and only slightly shorter than in germylenes **2**. As indicated by the frontier orbitals of **2** and **3** (Figure S32), the removal of chloride and addition of an electron to **2** results in enhanced π-type Ge–C back-bonding in the SOMO of **3** vs. the HOMO of **2**. However, since the SOMO of **3** is occupied by a single electron whereas the HOMO of **2** is occupied by two, the Ge–C bonds in **2** and **3** have comparable lengths.

The anions **4** and **5** can be chemically accessed by reaction of **2** with excess (2.2 equivalents) of $[K][C_{10}H_8]$ in THF or, alternatively, by direct reduction of **3** with KC_8 or $[K][C_{10}H_8]$ (Scheme 2). Solvate-free **4** and **5** were isolated by careful purification of the reaction products with pentane, while **4**·(THF) and **4**·$(THF)_2$ could be crystallised as a result from the presence of adventitious solvent molecules (Figures S28 and S29). The carbenic carbon signal appears at 226.3 ppm in the ^{13}C NMR spectrum of **4**, matching with literature data for **C** (212.1 ppm). This observation is reconciled by changes in the

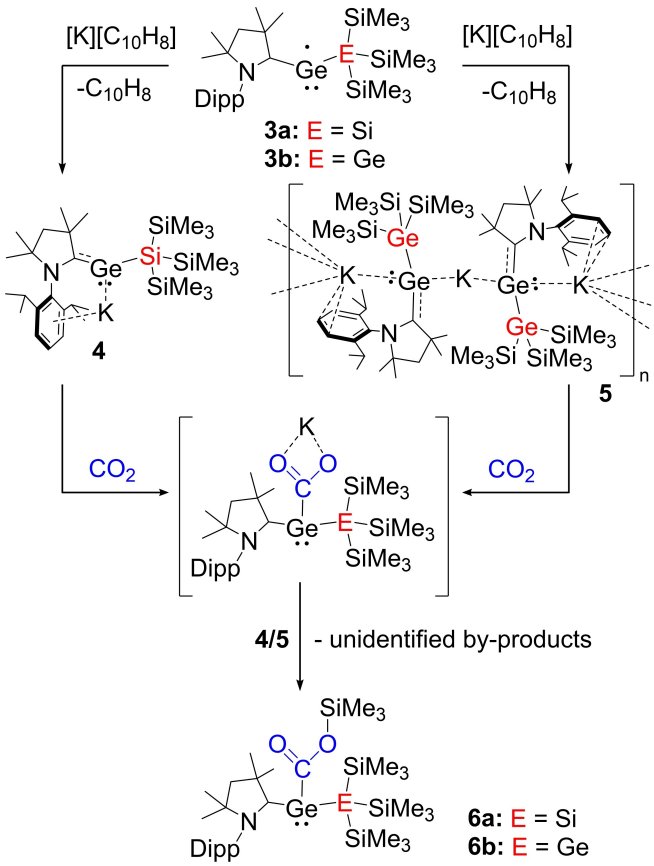

Scheme 2. Synthesis of anions **4** and **5**, and their reactivity with CO_2 to give complexes **6** (Dipp = 2,6-*i*$Pr_2C_6H_3$).

frontier orbitals of **2**, **3**, and **4** (Figure S32), and consistent with greater shielding relative to **2a** (248.0 ppm).

Unlike **C**, which exists as a dimer in the solid-state, complex **4** crystallizes as a discrete mononuclear species (Figure 2) that, however, forms pseudo-1D polymeric chains held together by anagostic C–H···K^+ interactions. In the crystal structure of **4**, the germanium atom is flanked by Me_2-cAAC and hypersilyl ligands, with potassium completing a trigonal planar coordination sphere. As suggested by the doubly occupied π-type HOMO of **4** (Figure S32), the Ge–C bond, 1.879(2) Å, is significantly shortened relative to **3a** (1.993(3) Å), while on par with that in **C** (1.874(2) Å). The Ge···K^+ distance in **4** (3.1878(6) Å) is considerably shorter than in **C** (3.2555(6) Å), indicating strong electrostatic interaction between the lone pair on germanium and potassium cation. The cation is further η^6-coordinated to the Dipp substituent and can readily participate in other coordinative interactions (the formation of **4**·(THF) and **4**·$(THF)_2$, see below).

Contrasting **4**, the solid-state structure of **5** depicts germanium in a pseudo-tetrahedral coordination environment with distortion towards disphenoidal (distorted tetrahedral) geometry (Figure 2). The long Ge···K^+ contacts (3.6253(7)–3.725(2) Å) work together with bridging K^+···(η^2-arene) interactions to connect adjacent complexes in 1-D helical chains (Figures S24 and S25). The extended structure of **5** arises, at least in part, from relaxed sterics, that is, from longer Ge–E bond distance (Ge1–Si1 = 2.4428(6) Å in **4** vs. Ge1–Ge2 = 2.5362(6) Å and Ge3–Ge4 = 2.5345(7) Å in **5**). The formation of 1-D chain structure of **5** is accompanied by elongation of the Ge–C bond relative to **4** (1.922(4) and 1.913(4) Å in **5** vs. 1.879(2) Å in **4**) due to attraction of the bridging potassium cation to electrons formally in the Ge–C π-bond and consequent enhancement of ylidone character on germanium (Scheme 3, right).

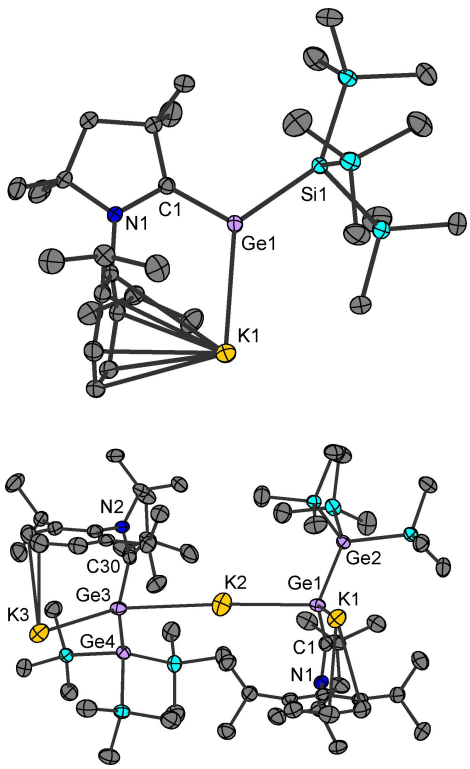

Figure 2. Solid-state structures of **4** (top) and asymmetric unit of **5** (bottom) with 50% probability ellipsoids. Full structural details for **4** and **5** are provided in the Supporting Information (Figures S22 and S23, respectively).

The ^{1}H NMR spectra of poorly soluble **5** (C_6D_6 and THF-d_8) show visible broadening, indicating that an extended structure is present also in solution. The broad resonances can, however, be resolved by introducing stoichiometric amounts of bis(2-methoxyethyl) ether (diglyme) to NMR solutions of **5**, yielding spectra that are comparable to those measured for **4** (Figure S7). The resolved solution NMR spectra of **5** show signals for free diglyme and adducts **5**·(diglyme) and $(\mathbf{5})_2$·(diglyme) could be crystallographically identified (Figures S30 and S31). This supports decomposition of the extended structure of **5** to a dynamic equilibrium of monomeric and dimeric subunits upon addition of diglyme.

The electronic structures of **4** and monomeric **5** were analysed by computational methods. The Ge–C bond has significant double bond character arising from π-type Ge–C back-bonding, as evidenced by the calculated Wiberg Bond Indices (WBIs) for the series **2a**, **3a**, **4**, and **5**: 1.04, 1.04, 1.44, and 1.45, respectively (Figure S34). For comparison, the WBI of the corresponding Ge–C bond in **C** is 1.40,[45] while that of each of the two equivalent Ge–C bonds in the germylone **A** is 1.15.[55] Natural population analyses of **4** and **5** reveal a highly electron rich germanium centre with a negative partial charge of −0.21 and −0.17 *e*, respectively; cf. +0.16 *e* in **C** and +0.33 *e* in the germylone **A**.[45,55] Subsequent Natural Bond Orbital (NBO) analyses found the ylidene description (Scheme 3, left) to be the best single Lewis-type depiction of the electronic structure of both **4** and monomeric **5**. However, a more detailed inspection of NBOs revealed the Ge–C π*-orbital in **4** and monomeric **5** to be occupied by as much as 0.23 *e*, indicating deviation from the ideally localised Lewis-model. In similar fashion, Electron Localization Function (ELF) analyses (Figure S35) further emphasised the importance of delocalization effects and the ylidone description for **4** and monomeric **5** (Scheme 3, right) by showing a significant flux of electrons between the monosynaptic V(Ge) lone pair basin and the disynaptic V(Ge,C) bond basin, each occupied on average by approximately three electrons. Taken as a whole, the electronic structures of **4** and monomeric **5** are between those of the two extremes shown in Scheme 3, and the Ge–C π-electrons can be viewed as an electron pair reservoir that is readily accessed by germanium to effect nucleophilicity. This behaviour parallels with that observed by Roesky in cAAC supported phosphini-

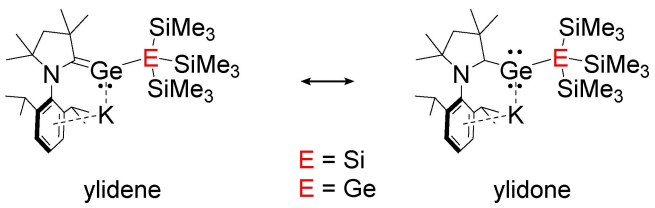

Scheme 3. Extreme ylidene and ylidone resonance descriptions of **4** and monomeric **5**.

denes/phosphaalkenes, and emphasizes the valence-isoelectronic relationship between (cAAC)PR and [(cAAC)GeR]$^-$ (R = organic substituent).[45,56]

The importance of the ylidone resonance form in the chemistry of **4** and **5** is best exemplified by their reactions with weak electrophiles, such as CO_2. Under 1 atm of CO_2, solutions of **4** and **5** undergo an instantaneous colour change from red to purple. Reaction atmospheres were subsequently degassed to limit deleterious side reactivity. After work-up, single crystal X-ray diffraction analysis revealed the products to be isostructural μ-CO_2-κ*C*:κ*O* complexes **6** (Scheme 2 and Figure 3). The concomitant intermolecular silyl group transfer eventuates low isolated yields (~20%). ^{13}C NMR shows carbenic carbon resonances at 246.5 and 247.8 ppm for **6a** and **6b**, respectively, matching those measured for **2a** and **2b**. Characteristic ν_{CO} stretches are observed in the IR spectra of **6a** and **6b** at 1613 and 1614 and cm^{-1}, respectively.

Computational analysis of the reaction mechanism suggested that CO_2 initially binds to the electrons flowing from the Ge–C π-bond in **4** and **5** in η^1-CO_2-κ*C* fashion. Subsequent migration of the potassium cation yields intermediate complexes exhibiting a μ$_2$-κC:κ^2*O,O′* bonding mode (Scheme 2 and Figure S36). The calculated gas phase reaction energies were found to be exothermic by ~50 kJ mol^{-1} but become approximately energy neutral upon inclusion of entropy terms and solvent effects. This is not unexpected as η^1-CO_2-κ*C* adducts are extremely rare[57–63] and potassium cation is a weak Lewis acid, providing significantly less electronic stabilization to the bound CO_2 molecule than the silyl group in **6**.

The aforementioned observations implicate germanium as a nucleophile in the addition of CO_2 and are reminiscent of early reports on in situ prepared triorganogermanecarboxylates.[64–66] Complexes **6** are also rare examples of μ-CO_2-κ*C*:κ*O* bonding involving a heavy Group 14 element. The only other crystallographically characterised example for germanium is a [4+2] cycloadduct of 1,4-digermabenzene with CO_2 in which the two metalloid centres work in tandem as a Lewis acid and a base.[67] Germanium mediated CO_2 transformations typically involve insertion to a Ge–H bond to give Ge–O bound formic acid derivatives.[68–72] Other reported examples include the conversion of heavy Group 14 ketones to κ^{2}O,O′ bound carbonates in the presence of CO_2[36,73] and side-on insertion of CO_2 to the Ge–Ge single bond of a digermyne to give a bis(germylene) oxide after CO release.[74] The high nucleophilic character of germanium in **4** and **5** is highlighted by comparison with germylones **A** that have not been reported to react with CO_2. In agreement with these observations, or the lack thereof, computational analyses probing the potential energy surface of cAAC$_2$Ge and CO_2 failed to locate a stable adduct between the two.

To summarize, mononuclear germanylidene complex **4** and coordination polymer **5** bearing cAAC and hypermetallyl ligands were synthesised by stepwise reduction from germylene precursors **2** through stable and isolable germanium radicals **3**. The germanium atom in **4** and **5** is highly electron-rich, with electrons formally in the Ge–C π-bond readily available for forming new intermolecular interactions, as illustrated by computational analyses, the extended solid-state structure of **5**, and the reactivity of **4** and **5** towards CO_2. Bridged μ-CO_2-κ*C*:κ*O* adducts **6** were obtained that display a common binding mode for CO_2 in transition metal complexes but rare for germanium. The reported efforts expand the portfolio of known cAAC-stabilised germanylidene anions and demonstrate their utility as efficient single-site nucleophiles that surpass ylidones of type **A**. Further reactivity studies of **4** and **5** with small molecules are currently underway.

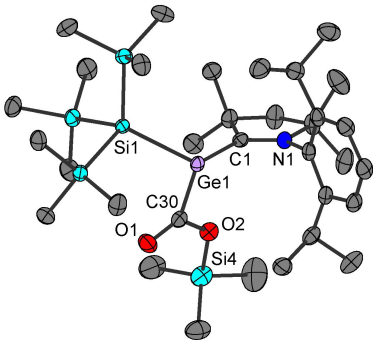

Figure 3. Solid-state structure of **6a** with 50% probability ellipsoids. Structural details for **6a** and isostructural **6b** are provided in the Supporting Information (Figure S26 and S27, respectively).

Experimental Section

Deposition Number(s) 2090119 (for **2a**), 2090120 (for **3a**), 2090121 (for **4**), 2090122 (for **4**·(THF)), 2090123 (for **4**·(THF)$_2$), 2090124 (for **6a**), 2090125 (for **2b**), 2090126 (for **3b**), 2090127 (for **5**), 2090128 (for (**5**)$_2$·(diglyme)), 2090129 (for **5**·(diglyme)) and 2090130 (for **6b**) contain(s) the supplementary crystallographic data for this paper. These data are provided free of charge by the joint Cambridge Crystallographic Data Centre and Fachinformationszentrum Karlsruhe Access Structures service.

Acknowledgements

Financial support for this work was provided by the University of Jyväskylä. This project has received funding from the European Research Council (ERC) under the European Union's Horizon 2020 research and innovation programme (grant agreement #772510 to H.M.T). Computational resources were provided by the Finnish Grid and Cloud Infrastructure (persistent identifier urn:nbn:fi:research-infras-2016072533).

Conflict of Interest

The authors declare no conflict of interest.

Keywords: donor-acceptor systems · germanium · main group elements · small molecule activation · sub-valent compounds

[1] S. S. Sen, H. W. Roesky, *Chem. Commun.* **2018**, *54*, 5046–5057.

[2] P. P. Samuel, A. P. Singh, S. P. Sarish, J. Matussek, I. Objartel, H. W. Roesky, D. Stalke, *Inorg. Chem.* **2013**, *52*, 1544–1549.
[3] K. A. Miller, J. M. Bartolin, R. M. O'Neill, R. D. Sweeder, T. M. Owens, J. W. Kampf, M. M. Banaszak Holl, N. J. Wells, *J. Am. Chem. Soc.* **2003**, *125*, 8986–8987.
[4] R. J. Mangan, A. Rit, C. P. Sindlinger, R. Tirfoin, J. Campos, J. Hicks, K. E. Christensen, H. Niu, S. Aldridge, *Chem. Eur. J.* **2020**, *26*, 306–315.
[5] T. Kunz, C. Schrenk, A. Schnepf, *Chem. Eur. J.* **2019**, *25*, 7210–7217.
[6] H. Jing, H. Ge, C. Li, Y. Jin, Z. Wang, C. Du, X. Fu, H. Fang, *Organometallics* **2019**, *38*, 2412–2416.
[7] Z. D. Brown, P. Vasko, J. C. Fettinger, H. M. Tuononen, P. P. Power, *J. Am. Chem. Soc.* **2012**, *134*, 4045–4048.
[8] S. R. Foley, G. P. A. Yap, D. S. Richeson, *J. Chem. Soc. Dalton Trans.* **2000**, 1663–1668.
[9] A. Jana, H. W. Roesky, C. Schulzke, *Dalton Trans.* **2009**, *39*, 132–138.
[10] Y. Peng, J.-D. Guo, B. D. Ellis, Z. Zhu, J. C. Fettinger, S. Nagase, P. P. Power, *J. Am. Chem. Soc.* **2009**, *131*, 16272–16282.
[11] J. Böserle, R. Jambor, A. Růžička, M. Erben, L. Dostál, *Dalton Trans.* **2020**, *49*, 4869–4877.
[12] D. F. Shriver, *Acc. Chem. Res.* **1970**, *3*, 231–238.
[13] J. Bauer, H. Braunschweig, R. D. Dewhurst, *Chem. Rev.* **2012**, *112*, 4329–4346.
[14] D. F. Shriver, *J. Am. Chem. Soc.* **1963**, *85*, 3509–3510.
[15] C. Gendy, A. Mansikkamäki, J. Valjus, J. Heidebrecht, P. C.-Y. Hui, G. M. Bernard, H. M. Tuononen, R. E. Wasylishen, V. K. Michaelis, R. Roesler, *Angew. Chem. Int. Ed.* **2019**, *58*, 154–158; *Angew. Chem.* **2019**, *131*, 160–164.
[16] S. Ishida, T. Iwamoto, C. Kabuto, M. Kira, *Nature* **2003**, *421*, 725–727.
[17] T. Iwamoto, T. Abe, C. Kabuto, M. Kira, *Chem. Commun.* **2005**, 5190–5192.
[18] T. Iwamoto, H. Masuda, C. Kabuto, M. Kira, *Organometallics* **2005**, *24*, 197–199.
[19] M. Kira, T. Iwamoto, S. Ishida, H. Masuda, T. Abe, C. Kabuto, *J. Am. Chem. Soc.* **2009**, *131*, 17135–17144.
[20] Y. Li, K. C. Mondal, H. W. Roesky, H. Zhu, P. Stollberg, R. Herbst-Irmer, D. Stalke, D. M. Andrada, *J. Am. Chem. Soc.* **2013**, *135*, 12422–12428.
[21] K. C. Mondal, H. W. Roesky, M. C. Schwarzer, G. Frenking, B. Niepötter, H. Wolf, R. Herbst-Irmer, D. Stalke, *Angew. Chem. Int. Ed.* **2013**, *52*, 2963–2967; *Angew. Chem.* **2013**, *125*, 3036–3040.
[22] Y. Xiong, S. Yao, S. Inoue, J. D. Epping, M. Driess, *Angew. Chem. Int. Ed.* **2013**, *52*, 7147–7150; *Angew. Chem.* **2013**, *125*, 7287–7291.
[23] Y. Xiong, S. Yao, G. Tan, S. Inoue, M. Driess, *J. Am. Chem. Soc.* **2013**, *135*, 5004–5007.
[24] B. Su, R. Ganguly, Y. Li, R. Kinjo, *Angew. Chem. Int. Ed.* **2014**, *53*, 13106–13109; *Angew. Chem.* **2014**, *126*, 13322–13326.
[25] T. Sugahara, T. Sasamori, N. Tokitoh, *Angew. Chem. Int. Ed.* **2017**, *56*, 9920–9923.
[26] Y. Wang, M. Karni, S. Yao, Y. Apeloig, M. Driess, *J. Am. Chem. Soc.* **2019**, *141*, 1655–1664.
[27] Y. Xiong, D. Chen, S. Yao, J. Zhu, A. Ruzicka, M. Driess, *J. Am. Chem. Soc.* **2021**, *143*, 6229–6237.
[28] S. Yao, A. Kostenko, Y. Xiong, C. Lorent, A. Ruzicka, M. Driess, *Angew. Chem. Int. Ed.* **2021**, *60*, 14864–14868; *Angew. Chem.* **2021**, *133*, 14990–14994.
[29] T. Chu, L. Belding, A. van der Est, T. Dudding, I. Korobkov, G. I. Nikonov, *Angew. Chem. Int. Ed.* **2014**, *53*, 2711–2715; *Angew. Chem.* **2014**, *126*, 2749–2753.
[30] Y.-P. Zhou, M. Karni, S. Yao, Y. Apeloig, M. Driess, *Angew. Chem. Int. Ed.* **2016**, *55*, 15096–15099; *Angew. Chem.* **2016**, *128*, 15320–15323.
[31] M. T. Nguyen, D. Gusev, A. Dmitrienko, B. M. Gabidullin, D. Spasyuk, M. Pilkington, G. I. Nikonov, *J. Am. Chem. Soc.* **2020**, *142*, 5852–5861.
[32] S. Roy, K. C. Mondal, L. Krause, P. Stollberg, R. Herbst-Irmer, D. Stalke, J. Meyer, A. C. Stückl, B. Maity, D. Koley, S. K. Vasa, S. Q. Xiang, R. Linser, H. W. Roesky, *J. Am. Chem. Soc.* **2014**, *136*, 16776–16779.
[33] B. Su, R. Ganguly, Y. Li, R. Kinjo, *Chem. Commun.* **2015**, *52*, 613–616.
[34] Y. Xiong, S. Yao, R. Müller, M. Kaupp, M. Driess, *Angew. Chem. Int. Ed.* **2015**, *54*, 10254–10257; *Angew. Chem.* **2015**, *127*, 10392–10395.
[35] Y. Xiong, S. Yao, M. Karni, A. Kostenko, A. Burchert, Y. Apeloig, M. Driess, *Chem. Sci.* **2016**, *7*, 5462–5469.
[36] A. Burchert, S. Yao, R. Müller, C. Schattenberg, Y. Xiong, M. Kaupp, M. Driess, *Angew. Chem. Int. Ed.* **2017**, *56*, 1894–1897; *Angew. Chem.* **2017**, *129*, 1920–1923.
[37] J. Hicks, P. Vasko, J. M. Goicoechea, S. Aldridge, *Nature* **2018**, *557*, 92–95.
[38] R. J. Schwamm, M. D. Anker, M. Lein, M. P. Coles, *Angew. Chem. Int. Ed.* **2019**, *58*, 1489–1493; *Angew. Chem.* **2019**, 131, 1503–1507.
[39] S. Grams, J. Eyselein, J. Langer, C. Färber, S. Harder, *Angew. Chem. Int. Ed.* **2020**, *59*, 15982–15986; *Angew. Chem.* **2020**, 132, 16116–16120.
[40] K. Koshino, R. Kinjo, *J. Am. Chem. Soc.* **2020**, *142*, 9057–9062.
[41] S. Kurumada, S. Takamori, M. Yamashita, *Nat. Chem.* **2020**, *12*, 36–39.
[42] R. J. Schwamm, M. P. Coles, M. S. Hill, M. F. Mahon, C. L. McMullin, N. A. Rajabi, A. S. S. Wilson, *Angew. Chem. Int. Ed.* **2020**, *59*, 3928–3932; *Angew. Chem.* **2020**, *132*, 3956–3960.
[43] J. Hicks, P. Vasko, J. M. Goicoechea, S. Aldridge, *Angew. Chem. Int. Ed.* **2020**, *60*, 1702–1713; *Angew. Chem.* **2021**, *133*, 1726–1737.
[44] M. M. Siddiqui, S. K. Sarkar, S. Sinhababu, P. N. Ruth, R. Herbst-Irmer, D. Stalke, M. Ghosh, M. Fu, L. Zhao, D. Casanova, G. Frenking, B. Schwederski, W. Kaim, H. W. Roesky, *J. Am. Chem. Soc.* **2019**, *141*, 1908–1912.
[45] M. M. Siddiqui, S. Sinhababu, S. Dutta, S. Kundu, P. N. Ruth, A. Münch, R. Herbst-Irmer, D. Stalke, D. Koley, H. W. Roesky, *Angew. Chem. Int. Ed.* **2018**, *57*, 11776–11780; *Angew. Chem.* **2018**, *130*, 11950–11954.
[46] J. D. Farwell, M. F. Lappert, C. Marschner, C. Strissel, T. D. Tilley, *J. Organomet. Chem.* **2000**, *603*, 185–188.
[47] D. Matioszek, N. Katir, S. Ladeira, A. Castel, *Organometallics* **2011**, *30*, 2230–2235.
[48] N. Katir, D. Matioszek, S. Ladeira, J. Escudié, A. Castel, *Angew. Chem. Int. Ed.* **2011**, *50*, 5352–5355; *Angew. Chem.* **2011**, *123*, 5464–5467.
[49] S. P. Mallela, S. Hill, R. A. Geanangel, *Inorg. Chem.* **1997**, *36*, 6247–6250.
[50] B. Cordero, V. Gómez, A. E. Platero-Prats, M. Revés, J. Echeverría, E. Cremades, F. Barragán, S. Alvarez, *Dalton Trans.* **2008**, 2832–2838.
[51] A. Poater, F. Ragone, S. Giudice, C. Costabile, R. Dorta, S. P. Nolan, L. Cavallo, *Organometallics* **2008**, *27*, 2679–2681.
[52] A. Poater, B. Cosenza, A. Correa, S. Giudice, F. Ragone, V. Scarano, L. Cavallo, *Eur. J. Inorg. Chem.* **2009**, *2009*, 1759–1766.
[53] A. Poater, F. Ragone, R. Mariz, R. Dorta, L. Cavallo, *Chem. Eur. J.* **2010**, *16*, 14348–14353.
[54] L. Falivene, Z. Cao, A. Petta, L. Serra, A. Poater, R. Oliva, V. Scarano, L. Cavallo, *Nat. Chem.* **2019**, *11*, 872–879.
[55] D. M. Andrada, N. Holzmann, G. Frenking, *Can. J. Chem.* **2016**, *94*, 1006–1014.
[56] S. Roy, K. C. Mondal, S. Kundu, B. Li, C. J. Schürmann, S. Dutta, D. Koley, R. Herbst-Irmer, D. Stalke, H. W. Roesky, *Chem. Eur. J.* **2017**, *23*, 12153–12157.
[57] G. Fachinetti, C. Floriani, P. F. Zanazzi, *J. Am. Chem. Soc.* **1978**, *100*, 7405–7407.
[58] S. Gambarotta, F. Arena, C. Floriani, P. F. Zanazzi, *J. Am. Chem. Soc.* **1982**, *104*, 5082–5092.
[59] J. C. Calabrese, T. Herskovitz, J. B. Kinney, *J. Am. Chem. Soc.* **1983**, *105*, 5914–5915.
[60] H. Tanaka, H. Nagao, S. M. Peng, K. Tanaka, *Organometallics* **1992**, *11*, 1450–1451.
[61] H. Tanaka, B. C. Tzeng, H. Nagao, S. M. Peng, K. Tanaka, *Inorg. Chem.* **1993**, *32*, 1508–1512.
[62] C. Yoo, Y. Lee, *Chem. Sci.* **2016**, *8*, 600–605.
[63] D. Oren, Y. Diskin-Posner, L. Avram, M. Feller, D. Milstein, *Organometallics* **2018**, *37*, 2217–2221.
[64] A. G. Brook, H. Gilman, *J. Am. Chem. Soc.* **1954**, *76*, 77–80.
[65] A. G. Brook, H. Gilman, *J. Am. Chem. Soc.* **1955**, *77*, 2322–2325.
[66] O. W. Steward, J. E. Dziedzic, J. S. Johnson, *J. Org. Chem.* **1971**, *36*, 3475–3480.
[67] T. Sugahara, J.-D. Guo, D. Hashizume, T. Sasamori, N. Tokitoh, *J. Am. Chem. Soc.* **2019**, *141*, 2263–2267.
[68] A. Jana, D. Ghoshal, H. W. Roesky, I. Objartel, G. Schwab, D. Stalke, *J. Am. Chem. Soc.* **2009**, *131*, 1288–1293.
[69] A. Jana, G. Tavčar, H. W. Roesky, M. John, *Dalton Trans.* **2010**, *39*, 9487–9489.
[70] G. Tan, W. Wang, B. Blom, M. Driess, *Dalton Trans.* **2014**, *43*, 6006–6011.
[71] T. J. Hadlington, C. E. Kefalidis, L. Maron, C. Jones, *ACS Catal.* **2017**, *7*, 1853–1859.
[72] N. Villegas-Escobar, H. F. Schaefer, A. Toro-Labbé, *J. Phys. Chem. A* **2020**, *124*, 1121–1133.
[73] D. Sarkar, C. Weetman, S. Dutta, E. Schubert, C. Jandl, D. Koley, S. Inoue, *J. Am. Chem. Soc.* **2020**, *142*, 15403–15411.
[74] J. Li, M. Hermann, G. Frenking, C. Jones, *Angew. Chem. Int. Ed.* **2012**, *51*, 8611–8614; *Angew. Chem.* **2012**, *124*, 8739–8742.

Manuscript received: August 2, 2021
Accepted manuscript online: August 17, 2021
Version of record online: ■■, ■■■■

COMMUNICATION

Stepwise reduction of germylenes via stable and isolable germanium radicals yields germanylidene anions supported by cyclic (alkyl)(amino) carbene and hypermetallyl ligands. The anions contain a highly electron-rich germanium centre with significant ylidone character and are efficient single-site nucleophiles that react even with weak electrophiles.

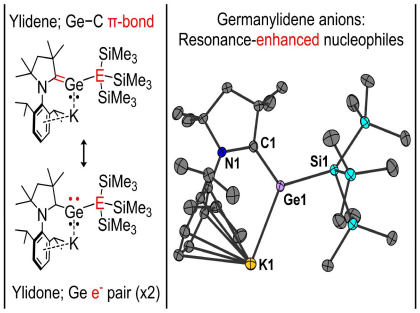

Dr. C. Gendy, Dr. J. Mikko Rautiainen, Dr. A. Mailman, Prof. Dr. H. M. Tuononen**